World Academy of Science, Engineering and Technology
International Journal of Chemical and Molecular Engineering
Vol:10, No:8, 2016

Investigation on Fischer-Tropsch Synthesis over Cobalt-Gadolinium Catalyst

Jian Huang, Weixin Qian, Haitao Zhang, Weiyong Ying

Abstract**—**Cobalt-gadolinium catalyst for Fischer-Tropsch synthesis was prepared by impregnation method with commercial silica gel, and its texture properties were characterized by BET, XRD, and TPR. The catalytic performance of the catalyst was tested in a fixed bed reactor. The results showed that the addition of gadolinium to the cobalt catalyst might decrease the size of cobalt particles, and increased the dispersion of catalytic active cobalt phases. The carbon number distributions for the catalysts was calculated by ASF equation.

Keywords**—**Fischer-Tropsch synthesis, cobalt-based catalysts, gadolinium, carbon number distributions.

I. Introduction

FISCHER-TROPSCH (FT) synthesis is a highly promising technology process for the production of lower olefins, clean liquid fuels, microcrystal waxes and other heavy hydrocarbons [1]. Production from synthesis gas through the FT synthesis process has attracted much attention in both catalysis and chemical engineering fields during 20th century, due to the potential of the technology providing an optional route for liquid fuel production and chemicals, which has played important parts in the modern economic development [2].

With the development of FT synthesis, lots of studies had shown that the introduction of noble metals (Ru, Rh, Pt, and Pd) has a strong influence on the structure and dispersion of cobalt species, FT synthesis reaction rates, and selectivities [3]-[7]. Promotion with oxides has been one of the methods to progress the activity and hydrocarbon selectivity of FT catalysts, especially among the oxide promoters, ZrO_2, La_2O_3, MnO, and CeO_2 have been extensively performed [8]-[11]. The Addition of oxide promoters could modify the catalyst texture and porosity, and increase cobalt dispersion, reducibility, and fraction of different cobalt metal crystalline phases [12], [13]. Addition of Gd to Co/SiO_2 catalysts increases the reducibility to Co metal, decreases CH_4 selectivity, and causes carbon deposition at lower temperatures when compared to the unpromoted catalyst [14].

FT synthesis processes involve stepwise incorporation of one carbon atom at a time with simultaneous formation of water, according to the overall equation:

$$n\,CO + 2n\,H_2 = (CH_2)_n + n\,H_2O \quad (1)$$

Jian Huang, Weixin Qian, Haitao Zhang, and Weiyong Ying are with the Engineering Research Center of Large Scale Reactor Engineering and Technology, Ministry of Education, State Key Laboratory of Chemical Engineering, the East China University of Science and Technology, ShangHai, 200237 China (e-mail: jhecust@hotmail.com, and wying@ecust.edu.cn).

The Aderson–Schluz–Flory (ASF) equation was established and recognized, which describes a phenomenon that the chain propagation and the termination probabilities are independent of carbon number, and the deviations from the ASF distribution were then attributed to experiment errors and artifacts [15], [16]. This model yields a linear plot of the logarithm of weight of product versus carbon number. However, lots of non-ASF distributions results show that the chain propagation and termination probabilities are not independent of carbon number [17], [18]. Dual site theory and particle size effect theory explain the non-ASF deviations [19].

The aim of this study is to investigate the catalytic performance over a cobalt catalyst modified by 2 wt.% Gd in a fixed bed reactor. Due to the tendency to generate linear long-chain hydrocarbons dominantly for cobalt-based catalyst, we just took alkanes into consideration and neglected aromatic compounds, alcohols and other oxygen containing compounds.

II. Experimental

A. Preparation of Catalysts

Supported cobalt catalyst was prepared using a commercially silica gel (1.7-2.4 mm), gadolinium nitrate (>98% Sinopharm Chemical Reagent Co., Ltd) and cobalt (II) nitrate hexahydrate (>99% Sinopharm Chemical Reagent Co., Ltd), via two-step impregnation method. Before the impregnation step, the SiO_2 support was calcined in air at 800 °C for 6 h. The support was impregnated using a certain concentration $Gd(NO_3)_3 \cdot 6H_2O$, kept at room temperature for 12 h. After the impregnation step, the catalyst was dried at 110 °C for 12 h, followed by calcination in air at 450 °C for 6 h. Then the SiO_2 supported cobalt was impregnated with 20 wt.% $Co(NO_3)_2 \cdot 6H_2O$, followed by dry and calcination under same conditions. The obtained catalyst was denoted as $CoGd/SiO_2$, and the catalyst without Gd was denoted as Co/SiO_2.

B. Characterization of Structured Catalysts

Nitrogen adsorption-desorption isotherms were obtained with a Micrometrics ASAP 2020 apparatus. Prior to N_2 adsorption, the samples were degassed under vacuum at 350 °C for 4 h. Specific surface areas were measured by Brunauer Emmet Teller (BET) method. Total pore volume and pore sizes were evaluated using the standard Barrett-Joyner-Halenda (BJH) treatment.

Powder x-ray diffraction (XRD) patterns were recorded on a Rigaku D/Max 2550 using Cu Kα radiation at 40 kV and 100 mA. XRD patterns were obtained over a 2θ range of 10-80° and a step size of 0.02°.

Hydrogen temperature-programmed reduction (H_2-TPR)

measurements were carried out on Micrometrics AutoChem II 2920. Prior to the H_2-TPR measurements, 0.050 g sample placed in a quartz U-tube reactor was pretreated in Ar stream at 350 °C for 1.0 h and then cooled to 50 °C. H_2-TPR was conducted with a gas mixture of 10 vol. % H_2 in Ar at a flow rate of 50 mL·min^{-1}. Temperature was raised to 800 °C with a heating rate of 10 °C·min^{-1}. Hydrogen consumption was measured by a thermal conductivity detector (TCD).

C. Test of Catalyst Performance

Catalyst performance was investigated in a fixed-bed reactor (ID 10 mm) with a stainless steel thermocouple tube embedded in catalyst bed. The loading weight of catalyst with particle size of 1.7-2.0 mm was 3.04 g, (5.00 ml). The activation of catalyst and FTS reaction was carried out in fixed bed in continuous H_2 and syngas, respectively. The reduction condition was under atmospheric pressure, 1000 h^{-1}, 400 °C and pure H_2 for 24 h. After cooling to 100 °C, the syngas with a certain molar ratio H_2/CO =2.0 was flowed into the system, the pressure was kept at 2.0 MPa in reaction system. The outlet of the reactor was connected with a hot trap (180 °C) and a cold trap (0 °C) for the separation of components with high and low boiling point respectively.

The products of FTS were separated into three portions: gas phase (tail gas), liquid phase (oil and water phase) and solid phase (wax phase). Two Agilent 7890A GCs with different columns and detectors are used for the analysis of products. CO, H_2, N_2, CO_2 and CH_4 are separated on 5A molecular sieve packed columns and Propack Q packed columns, then detected by two thermal conductivity detectors (TCDs) with pure He and H_2 as the carrier gas respectively. C_1-C_6 hydrocarbons in tail gas are separated on a HP-AL/S capillary column and detected with a flame ionization detector (FID) with N_2 as the carrier gas. The components in tail gas are quantified by standard gas containing CO, H_2, N_2, CO_2, CH_4 and C_1-C_6 hydrocarbons, with external standard method. The wax product from hot trap is dissolved in CS2 and analyzed on a DB-5ht capillary column, detected by FID (N_2 carrier gas). The oil product is separated on a HP-5 capillary column, detected by FID with N_2 as the carrier gas.

A stabilization period of more than 48 h is needed under the initial reaction condition in order to ensure the stable catalytic phases which can avoid the sharp change of crystalline structures observed by some scholars [20]. The experimental operating conditions were listed as follows: temperature 225 °C, pressure 2.0 MPa, space velocity 1000 h^{-1}, H_2/CO = 2.0, cumulative time 24 h. This study just took alkanes into consideration and neglected aromatic compounds, alcohols and other oxygen containing compounds. X_{CO} represents the conversion of CO and can be calculated by

$$X_{CO}(\%) = \frac{N_{CO,in} - N_{CO,out}}{N_{CO,in}} \times 100 \quad (2)$$

S_{Cn} represents the selectivity of C_n hydrocarbons and can be calculated by

$$S_{Cn}(\%) = \frac{n \bullet N_{Cn,out}}{N_{CO,in} - N_{CO,out}} \times 100 \quad (3)$$

WGS reaction can be calculated by:

$$S_{CO_2}(\%) = \frac{N_{CO_2,out}}{N_{CO,in} - N_{CO,out}} \times 100 \quad (4)$$

N is the mole flow rate (mol·h^{-1}), and n is the carbon number of hydrocarbons.

In ASF theory, the chain propagation is represented by [13], [14].

$$W_n / n = (1-\alpha)^2 \alpha^{n-1} \quad (5)$$

Also, it is more conveniently expressed in a logarithmic form:

$$\ln\left(\frac{W_n}{n}\right) = n \ln \alpha + \ln\left(\frac{(1-\alpha)^2}{\alpha}\right) \quad (6)$$

where W_n is the weight fraction of the product containing n carbons, and α is the probability of chain growth. This formula is only suitable for the FTS products on large crystallite metal catalysts.

III. Results and Discussion

The N_2 adsorption-desorption isotherms and the pore size distributions of the catalysts are shown in Fig. 1. All the isotherms present a typical type IV curve, which was characteristic of mesoporous material. The CoGd/SiO_2 catalyst retains one peak of pore size distribution that indicates the introduction of graphene was beneficial for the uniform pore size, compared with the CoGd/SiO_2 catalyst.

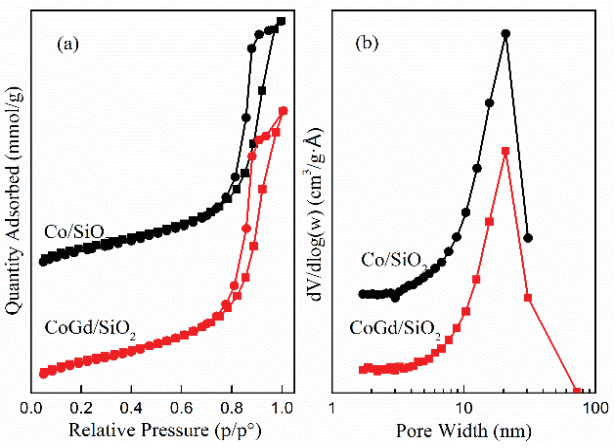

Fig. 1 (a) N_2 adsorption-desorption isotherms, and (b) pore size distributions

A brief compilation of the textural properties of the catalysts is presented in Table I. As observed, the surface area, pore volume and average pore diameter of the CoGd/SiO_2 had similar textural properties with Co/SiO_2 catalyst.

The XRD analysis of the cobalt catalysts was employed, as shown in Fig. 2, and it has shown that the XRD patterns of the catalysts with or without Gd have different peaks intensities. The noise levels have demonstrated that the carrier of catalysts is amorphous silica between 15 and 30° Bragg' angle. However, all of these two catalysts have the same phases, amorphous silica and cubic Co_3O_4.

TABLE I
SURFACE AREA, PORE VOLUME, AVERAGE PORE DIAMETER AND Co_3O_4 CRYSTAL SIZE FOR FRESH CALCINED CATALYSTS

Sample	S_{BET} ($m^2.g^{-1}$)	V_p[a] ($cm^3.g^{-1}$)	D_p[b] (nm)	D_{Co3O4}[c] (nm)
Co/SiO_2	169.7	0.392	11.4	22.9
$CoGd/SiO_2$	165.9	0.381	12.5	16.7

[a] BJH desorption pore volume.
[b] Adsorption average pore.
[c] Calculated from XRD using Scherrer equation

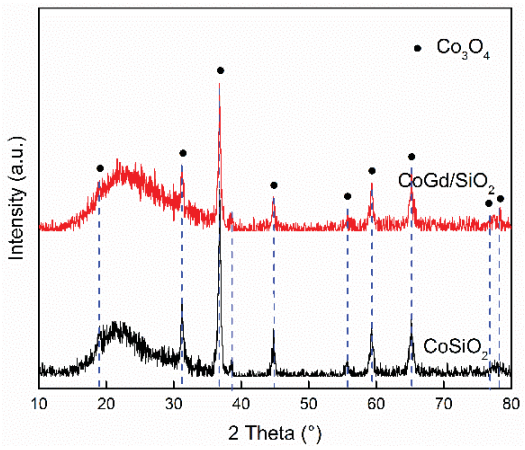

Fig. 2 XRD patterns of fresh calcined catalysts

Due to the addition of Gd to the cobalt catalyst, it was constituted by the particles with smaller sizes (Table I). This effect plays an important role in the evolution of the catalyst morphology, which might explain why in the case of the Gd, the size of particles decreased and CO_2 selectivity decreased with the addition of Gd to the catalyst, as shown in Table II. The WGS rate is determined by the formation of a formate intermediate species from adsorbed CO and dissociated hydrogen.

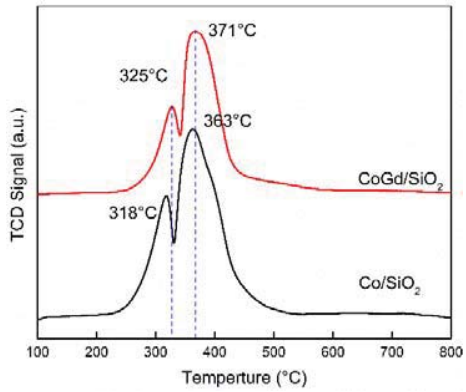

Fig. 3 TPR profiles of the two fresh calcined cobalt catalysts

The TPR profiles of cobalt catalysts are shown in Fig. 3. Two kinds of reduction behavior were observed. A pair of significantly resolved peaks observed in Fig. 3 reflects the reduction of cobalt oxide, Co_3O_4. Considering the hydrogen consumption, it is calculated that the first peak accounts for the reduction of Co^{3+} to Co^{2+} and the second peak for the reduction of Co^{2+} to cobalt. The peaks corresponding to the reduction temperature of $CoGd/SiO_2$ were increased distinctly, compared to the catalyst without Gd, respectively. The addition of Gd to the cobalt catalyst might decrease the size of cobalt particles from 22.9 nm to 16.7 nm in Table I, thus increasing the dispersion of catalytic active cobalt phases. This might favor the development of the chain growth reaction through the higher proportion of surface cobalt, resulting in a lower selectivity to CH_4.

TABLE II
FT SYNTHESIS RESULTS FOR THE COBALT CATALYSTS UNDER DIFFERENT TEMPERATURE[a]

Catalysts	Xco/%	S_{CO2} %	Selectivity[b] /%				
			C_1	C_2	C_3	C_4	C_5^+
Co/SiO_2	55.18	0.58	13.24	2.34	5.39	4.48	73.97
$CoGd/SiO_2$	49.83	0.27	11.62	1.44	4.03	3.35	79.29

[a]The catalytic activity and product selectivity data were calculated by averaging the values of 24 h.
[b]The data was based on mole carbon atom.

The results of the catalytic tests of $CoGd/SiO_2$ catalyst under FT synthesis conditions (at 2.0 MPa, 1000 h^{-1}, and 225 °C) are further summarized in Table II. It was observed that the conversion of CO was significantly decreased from 55.18 to 49.83% and also, the selectivity of methane was decreased from 13.24 to 11.62%, under the reaction conditions. A higher selectivity of long chain hydrocarbons (C_5^+) was obtained.

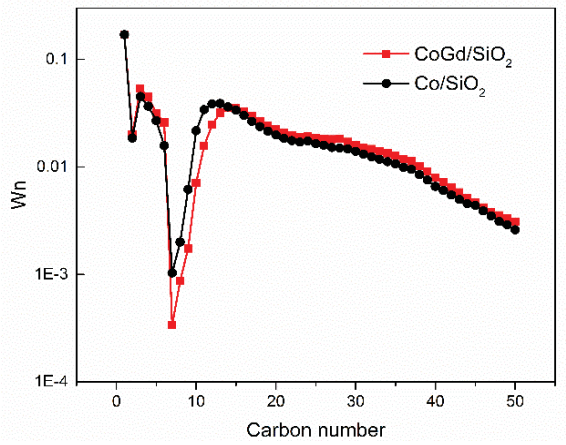

Fig. 4 Carbon number distributions of FT synthesis products

Carbon number distributions of FT synthesis products are presented in Fig. 4. According to ASF equation, a linear plot of the logarithm of weight fraction of product versus carbon number could be obtained. However, there is a phenomenon that two "breaks" are observed at C_2 and C_7, respectively. The deviation from the ASF distribution was interpreted by a preferable model of diffusion enhanced re-adsorption of

alkenes [21]. But ASF equation could not explain why different propagation probabilities were found on different carbon number products with the same catalyst. In fact, both dual site theory and particle size effect theory are intrinsically a mathematical fitting, which cannot explain why reaction conditions can affect product distributions on a certain catalyst.

IV. Conclusion

Cobalt catalyst modified by Gd was prepared by impregnation method, and its texture properties were characterized in more detail by BET, XRD, and TPR. The BET surface area and pore volume of $CoGd/SiO_2$ catalyst were slightly decreased, and the reduction temperature was appreciably increased, compared with Co/SiO_2 catalyst. The catalytic performance of $CoGd/SiO_2$ catalyst was tested and the results showed that the selectivity of methane and C_5^+ products on $CoGd/SiO_2$ catalyst was higher than that of Co/SiO_2 catalyst, but the CO conversion on $CoGd/SiO_2$ catalyst was lower compared with Co/SiO_2 catalyst. The addition of Gd to the cobalt catalyst might decrease the size of cobalt particles, and increased the dispersion of catalytic active cobalt phases.

Acknowledgment

The authors gratefully acknowledge the financial support of the National High-Tech R&D Program of China (2011AA05A204).

References

[1] Khodakov A. Y., Chu. W., Fongarland. P., "Advances in the development of novel cobalt Fischer-Tropsch catalysts for synthesis of long-chain hydrocarbons and clean fuels", *Chem. Rev.*, vol. 107, no. 5, pp. 1692-1744, 2007.

[2] Steynberg, A., & Dry, M. (Eds.), "Fischer-Tropsch Technology", Elsevier, 2004.

[3] Jacobs, G., Das, T. K., Zhang, Y., Li, J., Racoillet, G., & Davis, B. H., "Fischer–Tropsch synthesis: support, loading, and promoter effects on the reducibility of cobalt catalysts," Appl. Catal. A: Gen., vol. 233, no. 1, pp. 263-281, 2002.

[4] Reinikainen, M., Niemelä, M. K., Kakuta, N., & Suhonen, S., "characterisation and activity evaluation of silica supported cobalt and ruthenium catalysts", Appl. Catal. A: Gen., vol. 174, no.1, pp. 61-75, 1998.

[5] Qiu, X., Tsubaki, N., Sun, S., & Fujimoto, K., "Fischer–Tropsch synthesis: influence of noble metals on the performance of Co/SiO_2 catalyst for Fischer–Tropsch", *Fuel*, vol. *81*, pp. 1625-1630, 2002

[6] Ma, W., Jacobs, G., Keogh, R. A., Bukur, D. B., & Davis, B. H., "Fischer–Tropsch synthesis: Effect of Pd, Pt, Re, and Ru noble metal promoters on the activity and selectivity of a 25% Co/Al_2O_3", *Appl. Catal. A: Gen.*, vol. *437*, pp. 1-9, 2012.

[7] Chen, Li., Ying, W. Y., & Fang, D. Y., "Effect of component impregnation sequence on catalytic performance of Ru-Co-ZrO_2/γ-Al_2O_3 catalyst for Fischer-Tropsch synthesis", *Henan. Chem. Ind.*, vol. 25, pp. 16-19, 2008.

[8] Ma, W. P., Ding, Y. J., & Lin, L. W., "Fischer-Tropsch synthesis over activated-carbon-supported cobalt catalysts: effect of Co loading and promoters on catalyst performance", *Ind. Eng. Chem. Res.*, vol. *43, no.* 10, pp. 2391-2398, 2004.

[9] Haddad, G. J., Chen, B., & Goodwin Jr, J. G., "Effect of La^{3+} Promotion of Co/SiO2 on CO Hydrogenation", J. Catal., vol. 161, no. 1, pp. 274-281, 1996.

[10] Wei, M., Okabe, K., Arakawa, H., & Teraoka, Y., "Synthesis and characterization of zirconium containing mesoporous silicates and the utilization as support of cobalt catalysts for Fischer–Tropsch synthesis", *Catal. Commun.*, vol. 5, no. 10, pp. 597-603, 2004.

[11] Wang, T., Ding, Y., Xiong, J., Yan, L., Zhu, H., Lu, Y., & Lin, L., "Effect of vanadium promotion on activated carbon-supported cobalt catalysts in Fischer–Tropsch synthesis", Catal. Lett., vol. *107, no.* 1-2, pp. 47-52, 2006.

[12] Morales, F., de Groot, F. M., Gijzeman, O. L., Mens, A., Stephan, O., & Weckhuysen, B. M., "Mn promotion effects in Co/TiO_2 Fischer–Tropsch catalysts as investigated by XPS and STEM-EELS", *J. Catal.*, vol. 230, no. 2, pp. 301-308, 2005.

[13] Morales, F., de Groot, F. M., Glatzel, P., Kleimenov, E., Bluhm, H., Hävecker, M., ... & Weckhuysen, B. M., "In situ X-ray absorption of $Co/Mn/TiO_2$ catalysts for Fischer-Tropsch synthesis", J. Phys. Chem. B., vol. 108, no. 41, pp. 16201-16207, 2004.

[14] Huber, G. W., Butala, S. J., Lee, M. L., & Bartholomew, C. H. "Gd promotion of Co/SiO_2 Fischer–Tropsch synthesis catalysts", *Catal. Lett.*, vol. 74, no. 1-2, pp. 45-48, 2001

[15] Satterfield, C. N., & Huff, G. A., "Carbon number distribution of Fischer-Tropsch products formed on an iron catalyst in a slurry reactor", J. Catal., vol. 73, no. 1, pp. 187-197, 1982.

[16] Friedel, R. A., & Anderson, R. B., "Composition of Synthetic Liquid Fuels. I. Product Distribution and Analysis of C_5-C_8 Paraffin Isomers from Cobalt Catalyst", *J. Am. Chem. Soc.*, vol. 72, no. 3, pp. 1212-1215, 1950.

[17] Iglesia, E., Soled, S. L., & Fiato, R. A., "Fischer-Tropsch synthesis on cobalt and ruthenium. Metal dispersion and support effects on reaction rate and selectivity", J. Catal., vol. 137, no. 1, pp. 212-22, 1992.

[18] Huff, G. A., & Satterfield, C. N., "Evidence for two chain growth probabilities on iron catalysts in the Fischer-Tropsch synthesis", J. Catal., vol. 85, no. 2, pp. 370-379, 1984

[19] Yang, Y., Pen, S., & Zhong, B., "A new product distribution formulation for Fischer-Tropsch synthesis. Effect of metal crystallite size distribution", *Catal. Lett.*, vol. 16, no. 3, pp. 351-357, 1992.

[20] Qian, W., Zhang, H., Ying, W., & Fang, D., "The comprehensive kinetics of Fischer-Tropsch synthesis over a Co/AC catalyst on the basis of CO insertion mechanism". *Chem. Eng. J.,* vol. *228*, pp. 526-534, 2013.

[21] Madon, R. J., & Iglesia, E., "The importance of olefin readsorption and H_2/CO reactant ratio for hydrocarbon chain growth on ruthenium catalysts", *J. Catal.*, vol. 139, no. 2, pp. 576-590, 1993.